Investigation of Tungsten Unresolved Transition Array Spectrum around 300 Å for Fusion Plasma Diagnostics*)

Ryota NISHIMURA[1)], Tetsutarou OISHI[1)], Izumi MURAKAMI[2,3)], Daiji KATO[2,4)], Hiroyuki A. SAKAUE[2,3)], Gupta SHIVAM[5)], Hayato OHASHI[6)], Motoshi GOTO[2,3)], Yasuko KAWAMOTO[2,3)], Tomoko KAWATE[2,3)], Chihiro SUZUKI[2,3)], Hiroyuki TAKAHASHI[1)] and Kenji TOBITA[1)]

[1)]*Department of Quantum Science and Energy Engineering, Tohoku University, Sendai 980-8579, Japan*
[2)]*National Institute for Fusion Science, National Institutes of Natural Sciences, Toki 509-5292, Japan*
[3)]*The Graduate University for Advanced Studies, SOKENDAI, Toki 509-5292, Japan*
[4)]*Interdisciplinary Graduate School of Engineering Sciences, Kyusyu University, Kasuga 816-8580, Japan*
[5)]*Institute of Space and Plasma Sciences, National Cheng Kung University, Tainan 70101, Taiwan*
[6)]*Institute of Liberal Arts and Sciences, University of Toyama, Toyama 930-8555, Japan*

(Received 24 July 2024 / Accepted 18 September 2024)

Tungsten spectroscopic studies have attracted much attention, because tungsten will be used as a plasma-facing component in ITER and future DEMO reactors. However, spectral line data of tungsten ions in low to intermediate charge states, such as W^{8+}-W^{26+}, is still lacking. To accumulate spectral line data of W^{8+}-W^{26+}, it is very important to identify the charge state and transition of Unresolved Transition Array (UTA) spectrum, as well as discrete line spectrum. In this study, we investigated electron temperature dependence of a UTA spectrum around 300 Å for an advanced understanding of spectral line shape. As a result, the UTA spectrum contains W^{17+}-W^{27+} and emission line from 5s-5p transition and its satellite line from $5s^2$-5s5p transition are strongly emitted. It was suggested that the UTA spectrum around 300 Å will be useful for diagnostics of ITER edge plasma.

Keywords: Tungsten, EUV spectrum, spectroscopy, large helical device, flexible atomic code

DOI: 10.1585/pfr.20.2402005

1. Introduction

Tungsten (W) will be used as a plasma-facing component in divertor and first wall region in ITER and future DEMO reactors. Naturally, spectroscopic studies of tungsten impurities have attracted much attention. So far, tungsten spectroscopic studies have been performed in not only tokamaks, such as ASDEX Upgrade [1], JT-60U [2], JET [3], EAST [4], HL-2A [5], WEST [6], but also stellarators, such as TJ-II [7], and Large Helical Device (LHD) [8–10]. In addition to experimental studies, theoretical studies have also been performed using Collisional-Radiative (CR) model to identify the charge state and transition [11–13].

One of the current key issues is the lack of spectral line data, especially for tungsten ions in low to intermediate charge states, such as W^{8+}-W^{26+} [14]. In recent years, discrete lines from tungsten ions in low to intermediate charge state have been studied [15–17]. In contrast to discrete lines, Unresolved Transition Array (UTA) spectra, which have a quasi-continuum structure, around 15-45 Å [18], 45-70 Å [4, 18], 200 Å [19, 20], and 300 Å [21] have been observed. It was suggested that the UTA spectrum around 15-45 Å , 45-70 Å , 200 Å , and 300 Å contain W^{24+}-W^{33+}, W^{27+}-W^{45+}, W^{7+}-W^{27+}, and W^{14+}-W^{16+}, respectively. Among them, for advanced understanding of the UTA spectrum around 300 Å , it is very important to accumulate spectral shape data at different electron temperatures. Therefore, the purpose of this present paper is to observe the shape of the tungsten UTA spectrum around 300 Å with different electron parameters and to identify its detailed structure, i.e., ion charge state and transition.

2. Experimental Setup

Tungsten pellet injection experiments have been performed in LHD [22]. We used an Extreme UltraViolet (EUV) spectrometer called "EUV Long" [23], which covers 50-500 Å. In this present paper, the observation wavelength range and exposure time were set to 197.8-435.9 Å and 5 ms. Through the wavelength resolution depends on wavelength, it was evaluated to be 0.46 Å of full width at half maximum by Gaussian fitting of He II (303.78 Å). The configuration of pellet injection system and spectrometer is same as Ref. [24]. The waveforms of plasma heating power, central electron temperature, T_{e0}, central electron density, n_{e0}, plasma stored energy, W_p, and radiation

author's e-mail: nishimura.ryota.s5@dc.tohoku.ac.jp
*) This article is based on the presentation at the 26th International Conference on Spectral Line Shapes (ICSLS2024).

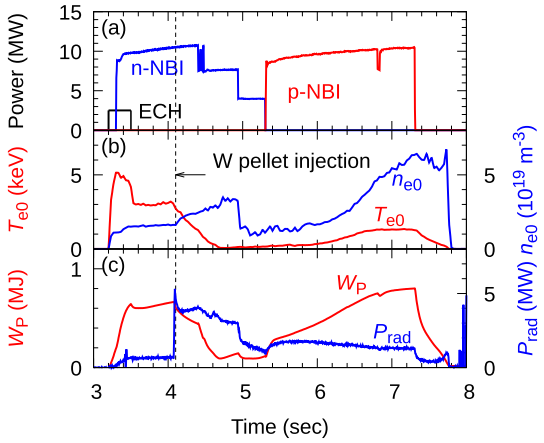

Fig. 1 Discharge waveforms of (a) plasma heating power, (b) central electron temperature, T_{e0} and central electron density, n_{e0}, and (c) plasma stored energy, W_p, and radiation power, P_{rad}.

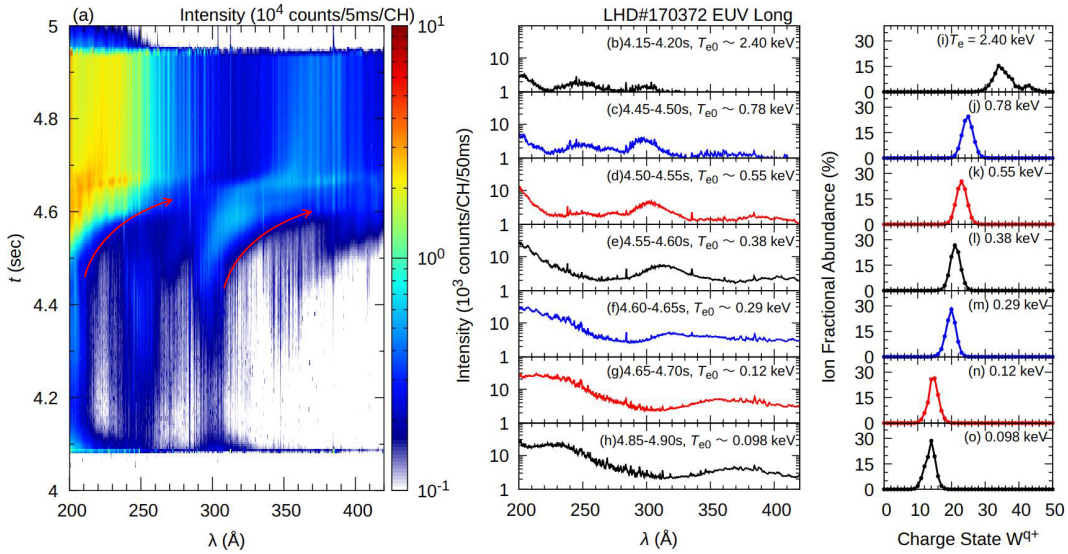

Fig. 2 (a) Time evolution of EUV spectrum, (b)-(h) EUV spectra taken in 4.20-4.90 s, (i)-(o) fractional abundance of W^{q+} ion density estimated using T_{e0}.

power, P_{rad} of tungsten pellet injection experiment, are shown in Figs. 1 (a)-(c).

Here, the T_{e0} and n_{e0} were measured by Thomson scattering diagnostics system [25], and the P_{rad} was measured by bolometer [26]. The discharge gas as well as Neutral Beam Injection (NBI) working gas was H_2. The plasma was ignited by Electron Cyclotron Heating (ECH), and maintained at $T_{e0} \sim 3.0$ keV and $n_{e0} \sim 1.5 \times 10^{19}$ m^{-3} by negative ion source NBI (n-NBI) before tungsten pellet injection ($t \sim 4.1$ s). After pellet injection, P_{rad} increased abruptly and then stabilized at a high level, while W_p gradually decreased. On the other hand, n_{e0} slightly increased from 1.5×10^{19} to 3×10^{19} m^{-3} due to ionization of tungsten, while T_{e0} decreased from 3.0 keV to a few hundred eV. During the discharge, a total of three n-NBIs are shut off one by one in stages, and switched to a total two of positive ion source NBIs (p-NBIs) at $t > 5.3$ s.

3. Observation and Identification of UTA Spectrum around 300 Å

Time evolution of observed EUV spectra taken in 4.20-4.90 s, and fractional abundance of W^{q+} ion density estimated using T_{e0} and ADF-11 data from OPEN-ADAS [27] are shown in Figs. 2 (a)-(h), 2 (i)-(o), respectively.

Two UTA spectra were observed at 200-250 Å and 290-400 Å after 4.20 s. Since the time evolution of these UTA spectra is similar, the UTA spectrum at 290-400 Å is composed by similar charge states to W^{7+}-W^{27+} of the UTA spectrum around 200 Å [19]. The UTA spectra shifted toward longer wavelength side with decreasing T_{e0}. This is thought to be due to a change in the charge state distribution at the lower electron temperature, as shown in Figs. 2 (i)-(o).

Then, we performed CR modeling for W^{17+}-W^{27+} using Flexible Atomic Code (FAC) version 1.1.5 [28], which is an integrated software package for calculation of en-

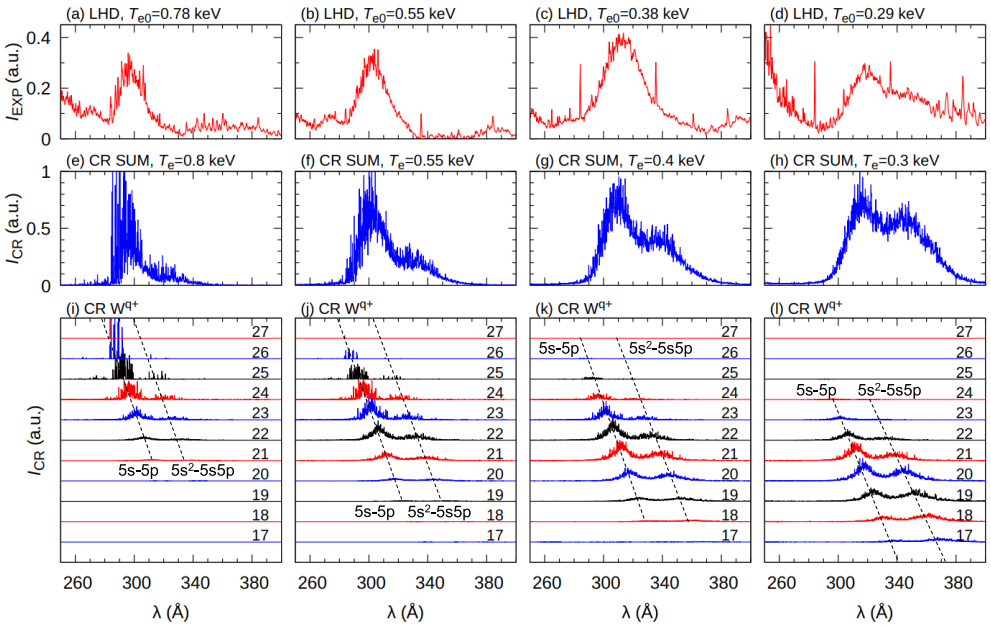

Fig. 3 (a)-(d) Observed EUV spectra at λ ~ 250 - 400 Å in LHD, (e)-(h) synthesized spectra of W^{17+}-W^{27+}, and (i)-(l) synthesized spectra of each ion.

ergy level, radiative transition rate, electron collision cross-section, based on a Relativistic Configuration Interaction (RCI) method using Dirac-Coulomb hamiltonian. We consider $4f^m$ (m=11-1), $4f^{m-1}$ nl ($m = 11-1, n = 5, 6, l \leq 4$), $4d^9 4f^{m+1}/4f^m 5s$ ($m = 11-1$), $4f^{m-2}5s^2/5s5p/5p^2/5s5d$ ($m = 11-2$) configurations. Then, the population density, N_i, was calculated as $dN_i/dt = \Gamma_{in} - \Gamma_{out} = 0$, where

$$\Gamma_{in} = \sum_{j>i}(A_{ji}N_j + C^d_{ji}n_e N_j) + \sum_{j<i} C^e_{ji} n_e N_j, \quad (1)$$

$$\Gamma_{out} = \sum_{j<i}(A_{ij}N_i + C^d_{ij}n_e N_i) + \sum_{j>i} C^e_{ij} n_e N_i + \sum_i C^i_i n_e N_i. \quad (2)$$

In the Eqs. (1) and (2), A_{ji}, C^d_{ji}, C^e_{ji}, and C^i_i represent radiative transition rate, rate coefficient of electron de-excitation, excitation, and ionization, respectively. Line emission intensity was calculated as $A_{ij}N_i\Delta E_{ij}$, where ΔE_{ij} represents the transition energy. An emission spectrum from W^{q+} was synthesized by involving all emission lines as a Gaussian distribution with a width of 0.02 eV. Since the ion density of W^{q+} was unknown, we used ion fractional abundance instead. Figures 3 (a)-(d), 3 (e)-(h), and 3 (i)-(l) show the observed EUV spectra at λ ~ 250 - 400 Å in LHD, synthesized spectra of W^{17+}-W^{27+}, and synthesized spectra of each ion, respectively.

Note that constant offset component of the spectra in Figs. 3 (a)-(d) were subtracted so that the minimum value of the intensity is almost zero. The spectra were calculated at a condition of $n_e = 10^{19}\,\mathrm{m}^{-3}$ and $T_e = 0.8, 0.55, 0.4$, and 0.3 keV. The synthesized spectra at $T_e = 0.8$, 0.55, 0.4, and 0.3 keV are drawn by blue line in Figs. 3 (e)-(h), and mainly consists of W^{22+}-W^{27+}, W^{20+}-W^{26+}, W^{19+}-W^{25+}, and W^{17+}-W^{23+}, respectively. The synthesized spectrum of each ion has two quasi-continuum peaks, which correspond to 5s-5p transition and its satellite line from $5s^2$-5s5p transition. The UTA spectrum shifts toward the longer wavelength side as the electron temperature decreases, and a structure with two quasi-continuous peaks becomes prominent, as overall. And the synthesized UTA spectrum reproduces the spectral shape of observed UTA spectrum in the tungsten pellet injection experiment. On the other hand, the observed spectrum and synthesized spectrum have some differences, for example, λ > 330 Å in Figs. 3 (a) and 3 (e), λ < 290 Å in Figs. 3 (d) and 3 (h). It is considered that the observed UTA spectrum contains ions in charge states lower than W^{17+}, which mainly distribute in outer side of the plasma. The central electron temperature was assumed in the calculation. Thus, it is necessary to consider the spatial distribution of electron temperature and ion density, in the future. The UTA spectrum around 300 Å will be useful for diagnostics of ITER edge plasma.

In this present paper, we conducted modeling of W^{17+}-W^{27+}. However, there are few spectral line data of tungsten ions below W^{17+}. In the future, identification of tungsten spectra from ions in lower charge states through high-temperature plasma and Electron Beam Ion-Trap (EBIT) experiments and theorical calculations is a key theme for fusion plasma diagnostics.

4. Summary

We observed tungsten UTA spectra around 300 Å by tungsten pellet injection experiment in LHD. The observed UTA spectrum shifted toward longer wavelength side with decreasing T_{e0} from 0.8 keV to 0.3 keV. The UTA spec-

trum of W^{17+}-W^{27+} synthesized using CR model reproduced the shape of observed spectra, as well as the peak wavelength. It is considered that the UTA spectra around 300 Å will be useful for diagnostics of ITER edge plasma.

Acknowledgments

The authors thank all the members, including technical staff, of the LHD team for their efforts to support the experiment in LHD. This work was partially supported by JSPS KAKENHI (Grant Numbers JP20K03896 and JP21H04460), the NIFS Collaboration Research program (Grant Numbers NIFS23KIPP031, NIFS23KIIP021, and NIFS23KIPF007), and JST, the establishment of university fellowships towards the creation of science technology innovation, Grant Number JPMJFS2102. The data supporting the findings of this study are available in the LHD experiment data repository at https://doi.org/10.57451/lhd.analyzed-data.

[1] K. Amsmussen *et al.*, Nucl. Fusion **38**, 967 (1998).
[2] T. Nakano and The JT-60 Team, J. Nucl. Mater. **415**, S327 (2011).
[3] G.J. van Rooij *et al.*, J. Nucl. Mater. **438**, S42 (2013).
[4] L. Zhang *et al.*, Nucl. Instrum. Methods Phys. Res. A **916**, 169 (2019).
[5] C. Dong *et al.*, Nucl. Fusion **59**, 016020 (2019).
[6] R. Guirlet *et al.*, Plasma Phys. Control. Fusion **64**, 105024 (2022).
[7] B. Zurro *et al.*, Plasma Phys. Control. Fusion **56**, 124007 (2014).
[8] T. Oishi *et al.*, Phys. Scr. **91**, 025602 (2016).
[9] T. Oishi *et al.*, Phys. Scr. **96**, 025602 (2021).
[10] T. Oishi *et al.*, Atoms **9**, 69 (2021).
[11] H.A. Sakaue *et al.*, Phys. Rev. A **92**, 012504 (2015).
[12] W. Li *et al.*, Phys. Rev. A **91**, 062501 (2015).
[13] I. Murakami *et al.*, Nucl. Mater. Energy **26**, 100923 (2021).
[14] A. Kramida *et al.*, http://physics.nist.gov/asd for NIST Atomic Spectra Database (Ver. 5.10).
[15] M. Mita *et al.*, J. Phys.: Conf. Ser. **875**, 012019 (2017).
[16] Priti *et al.*, Atoms **11**, 57 (2023).
[17] S. Murata *et al.*, X-ray spectrometry **49**, 200 (2019).
[18] Y. Liu *et al.*, J. Appl. Phys. **122**, 233301 (2017).
[19] C. Suzuki *et al.*, J. Phys. B: At. Mol. Opt. Phys. **44**, 175004 (2011).
[20] R. Nishimura *et al.*, submitted to Nucl. Mater. Energy.
[21] K.J. McCarthy *et al.*, Phys. Scr. **91**, 115601 (2016).
[22] Y. Takeiri *et al.*, Nucl. Fusion **57**, 102023 (2017).
[23] B. Chowdhuri *et al.*, Rev. Sci. Instrum. **78**, 1122 (2001).
[24] R. Nishimura *et al.*, Plasma Fusion Res. **19**, 1402022 (2024).
[25] N. Narihara *et al.*, Rev. Sci. Instrum. **72**, 1122 (2001).
[26] B. Peterson *et al.*, Fusion Sci. Technol. **58**, 412 (2010).
[27] H.P. Summers, The ADAS User Manual version 2.6, http://www.adas.ac.uk (2004).
[28] M.F. Gu *et al.*, Astrophys. J. **582**, 1241 (2003).